

Article

Not peer-reviewed version

CMAG: A Mission to Study and Monitor the Inner Corona Magnetic Field

[David Orozco Suárez](#)*, Jose Carlos Del Toro Iniesta, [Francisco Javier Bailén Martínez](#), María Balaguer, Daniel Álvarez García, [Daniel Serrano](#), Luis F. Peñín, [Alicia Vázquez-Ramos](#), Luis Ramón Bellot Rubio, Julia Atienzar, [Isabel Pérez Grande](#), [Ignacio Torralbo Gimeno](#), [Esteban Sanchis-Kilders](#), Jose Luis Gasent Blesa, [David Hernández Expósito](#), [Basilio Ruiz Cobo](#), Javier Trujillo Bueno, [R. Erdelyi](#), [J. A. Davies](#), Lucie M. Green, Sarah Matthews, David Long, [Michail Mathioudakis](#), [Christian Kintzinger](#), Jorrit Leenaarts, Silvano Fineschi, [Eamon Scullion](#)

Posted Date: 26 October 2023

doi: 10.20944/preprints202310.1715.v1

Keywords: Sun: corona; Sun: magnetic field; instrumentation: polarimeters; radiative transfer












Preprints.org is a free multidiscipline platform providing preprint service that is dedicated to making early versions of research outputs permanently available and citable. Preprints posted at Preprints.org appear in Web of Science, Crossref, Google Scholar, Scilit, Europe PMC.

Copyright: This is an open access article distributed under the Creative Commons Attribution License which permits unrestricted use, distribution, and reproduction in any medium, provided the original work is properly cited.

Article

CMAG: A Mission to Study and Monitor the Inner Corona Magnetic Field

Orozco Suárez, D.^{1,2} , del Toro Iniesta, J. C.^{1,2} , Bailén Martínez, F. J.^{1,2} , Balaguer Jiménez, M.^{1,2}, Álvarez García, D.^{1,2}, Serrano, D.³, Peñín, L.F.³, Vázquez Ramos, A.⁴, Bellot Rubio, L.R.^{1,2} , Atienzar, J.^{1,2}, Pérez Grande, I.^{2,5}, Torralbo Gimeno, I.^{2,5}, Sanchis Kilders, E.^{2,6}, Gasent Blesa, J.L.^{2,6}, Hernández Expósito, D.^{2,7}, Ruiz Cobo, B.^{2,7}, Trujillo Bueno, J.^{7,8,9}, Erdélyi, R.^{10,11,12} , Davies, J.A.¹³, Green, L.M.¹⁴ , Matthews, S.A.¹⁴ , Long, D.M.¹⁵ , Mathioudakis, M.¹⁵, Kintziger, C.¹⁶ , Leenaarts, J.¹⁷, Fineschi, S.¹⁸, Scullion E.¹⁹

¹ Instituto de Astrofísica de Andalucía (IAA-CSIC), Apdo. de Correos 3004, E-18080 Granada, Spain

² Spanish Space Solar Physics Consortium (S³PC)

³ SENER Aerospace, Severo Ochoa 4, 28760 Tres Cantos, Madrid, Spain

⁴ Departamento de Física Teórica y del Cosmos (DFTC) - Universidad de Granada (UGR) Campus de Fuentenueva, E-18071 Granada, Spain

⁵ Instituto de Microgravedad "Ignacio da Riva" (IDR-UPM), Plaza Cardenal Cisneros 3, E-28040 Madrid, Spain

⁶ Universitat de València Estudi General (UEVG), Avda. de la Universitat s/n, E-46100 Burjassot, Spain

⁷ Instituto de Astrofísica de Canarias, Vía Láctea, s/n, E-28080 La Laguna, Spain

⁸ Departamento de Astrofísica, Facultad de Física, Universidad de La Laguna, Tenerife, Spain

⁹ Consejo Superior de Investigaciones Científicas, Spain

¹⁰ Solar Physics & Space Plasma Research Center (SP2RC), School of Mathematics and Statistics, University of Sheffield, Hounsfield Road, Sheffield, S3 7RH, UK; robertus@sheffield.ac.uk

¹¹ Department of Astronomy, Eötvös Loránd University, Pázmány Péter sétány 1/A, Budapest H-1117, Hungary

¹² Gyula Bay Zoltan Solar Observatory (GSO), Hungarian Solar Physics Foundation (HSPF), Petőfi tér 3., Gyula H-5700, Hungary.

¹³ STFC-RAL Space, Harwell Campus, Didcot, Oxfordshire, OX11 0QX, UK

¹⁴ Mullard Space Science Laboratory, UCL, Dorking, Surrey, UK

¹⁵ Astrophysics Research Centre, School of Mathematics and Physics, Queen's University Belfast, University Road, Belfast, BT7 1NN, Northern Ireland, UK,

¹⁶ Centre Spatial de Liège, University of Liège (ULiège) – STAR Institute

¹⁷ Institute for Solar Physics, Department of Astronomy, Stockholm University, AlbaNova University Centre, SE-106 91 Stockholm, Sweden

¹⁸ INAF - Osservatorio Astrofisico di Torino (Italy)

¹⁹ Northumbria University, NE1 8ST Newcastle upon Tyne, UK

* Correspondence: orozco@iaa.es

Abstract: Measuring magnetic fields in the inner corona, the interface between the solar chromosphere and outer corona, is of paramount importance if we aim at understanding the energetic transformations taking place there and which is at the origin of processes that lead to coronal heating, solar wind acceleration, and of most of the phenomena relevant to space weather. However, these measurements are more difficult than mere imaging because polarimetry requires differential photometry. The Coronal Magnetograph mission (CMAG) has been designed to map the vector magnetic field, line-of-sight velocities, and plane-of-the-sky velocities of the inner corona with unprecedented spatial and temporal resolutions from space. This will be achieved through full vector spectropolarimetric observations using a coronal magnetograph as the sole instrument on board a spacecraft, combined with an external occulter installed on another spacecraft. The two spacecraft will maintain a formation flight distance of 430 meters for coronagraphic observations, which requires a 2 m occulter disk radius. The mission will be preferentially located at the Lagrangian L5 point, offering a significant advantage for solar physics and space weather research. Existing ground-based instruments face limitations such as atmospheric turbulence, solar scattered light, and long integration times when performing coronal magnetic field measurements. CMAG overcomes these limitations by performing spectropolarimetric measurements from space with an external

occulters and high-image stability maintained over time. It achieves the necessary sensitivity and offers a spatial resolution of 2.5 arcseconds and a temporal resolution of approximately one minute, in its nominal mode, covering the range from 1.02 solar radii to 2.5 radii. CMAG relies on proven European technologies and can be adapted to enhance any other solar mission, offering potential significant advancements in coronal physics and space weather modeling and monitoring.

Keywords: Sun: corona; Sun: magnetic field; instrumentation: polarimeters; radiative transfer

1. Introduction

1.1. State-of-the-art in coronal science

The solar corona, extending from the transition region into the heliosphere, exhibits fascinating characteristics that challenge our current understanding. The temperature of the corona rises rapidly in its lower layers, reaching temperatures of a few million Kelvin, while the gas pressure decreases sharply through the transition region, maintaining a relatively constant level further out. Within the inner corona, complex magnetic fields give rise to highly structured, bright features known as streamers and coronal loops. These structures, influenced by the solar dynamo and activity cycle, remain enigmatic in terms of their magnetic properties.

Coronal loops, in particular, are hotter and denser than the surrounding plasma, yet the mechanisms responsible for their heating and filling remain elusive [34]. The overall high temperature of the global corona itself also poses a significant mystery. Unraveling the processes of coronal heating is considered a paramount challenge in solar physics. The lack of knowledge about the magnetism of the inner corona further complicates our understanding of these phenomena. This region of the corona hosts intricate magnetic field reconnection processes, leading to the generation of flares and energetic particle events across a broad range of scales.

Flares emit radiation across various wavelengths, from radio waves to hard X-rays and even gamma-rays. Many large flares are accompanied by coronal mass ejections (CMEs), which are the primary sources of space weather effects on Earth, potentially triggering severe geomagnetic storms [42]. CMEs also generate powerful shock waves as the plasma expands during their formation and propagation through the corona. Additionally, a multitude of magnetohydrodynamic (MHD) waves can be observed propagating upward into the heliosphere within the inner corona [11,29]. It is evident that magnetic fields play a crucial role in governing all aspects of the inner solar corona, driving the solar wind and influencing space weather phenomena. However, the detailed properties of these magnetic fields remain largely unexplored [2].

The CMAG mission offers an opportunity to address key questions related to the coronal heating problem, flare and CME formation, and the generation and energy transport of waves. By providing fundamental data on the vector magnetic field and velocity measurements of the inner corona at unprecedented spatial and temporal resolutions, CMAG would enable substantial advancements in coronal models beyond existing empirical approximations. Moreover, it would contribute to more accurate space weather predictions, ultimately enhancing our understanding of the Sun and its influence on the heliosphere, the Earth's environment and our technological systems and society.

1.2. Observing the inner solar corona

Observing the inner solar corona presents a significant challenge primarily due to the faintness of the emitted light from the coronal material compared to the overall brightness of the Sun. Consequently, observing the solar corona requires blocking the light emitted by the solar disk. This can be accomplished during a solar eclipse, which only lasts for a few minutes, or through the use of specialized instruments called coronagraphs. However, the solar coronal light becomes intermingled

with background signals originating from scattered light, mainly from the occulter, but also from the instrument optics. Despite these difficulties, extensive efforts have been made to carry out coronal observations using both ground- and space-based assets.

Instruments for coronal observations include LASCO [5] and UVCS [21], both aboard SoHO [10]; STEREO/SECCHI [14]; METIS [1] and SoloHI [15] on Solar Orbiter [30]; WISPR [49] onboard the Parker Solar Probe [33]; ASPIICS [13] on Proba-3; the High-Altitude Observatory (HAO)/National Center for Atmospheric Research (NCAR) Coronal Multichannel Polarimeter (CoMP) [43] and the upgraded version uCoMP [44]; CRYO-NIRSP [12] on DKIST [36]. However, while imaging the corona poses challenges, determining its magnetic field is even more difficult due to the need for differential photometry to measure the four Stokes parameters of polarized light. The aforementioned ground-based instruments, uCoMP and CRYO-NIRSP, have capabilities for magnetic field measurements and provide valuable insights into coronal dynamics, which is known to be driven by the conversion of magnetic energy into radiative energy (in the case of flares) and the kinetic energy of material (in the case of coronal mass ejections or CMEs). Nevertheless, these measurements are significantly hampered by atmospheric turbulence, solar scattered light, and long integration times, resulting in a limited understanding of the intricate details of these energy transformations. However, new diagnostics emerge that can provide insights into the magnetic fields of the inner corona. For instance, a newly developed diagnostic technique that involves atomic radiation modeling of the contribution of a magnetically induced transition to the Fe X 25.7262 nm spectral line intensity, has been presented in [20,25,26] and used, later, to obtain the magnetic field in active region loops [4] using Hinode [22] Extreme-ultraviolet Imaging Spectrometer EIS [7]. More recently, Yang and collaborators [50] presented a method that utilizes spectroscopic measurements and MHD assumptions to indirectly estimate the strength of the coronal magnetic field. These techniques may be very useful in the future, in the context of other space missions such as SPARK [35]. However, what is truly needed is direct observation of the polarization signals associated with the magnetic field (see a review in [47]). In this respect, it is of interest to note that in 2015 the Chromospheric Lyman-Alpha Spectro-Polarimeter (CLASP) mission obtained the first observations of the linear polarization due to scattering processes in the hydrogen Lyman-alpha line of the solar-disk radiation, while in 2019 and 2021 the Chromospheric Layer Spectro-Polarimeter (CLASP2 and CLASP2.1) missions obtained unprecedented observations of the linear and circular polarization signals caused by scattering processes and the Hanle and Zeeman effects in the near-UV region of the Mg II h & k lines. These suborbital space experiments have opened a window for probing the magnetism and geometry of the plasma in the upper chromosphere and transition region of the Sun [47].

The CMAG mission aims to overcome the aforementioned limitations by observing the inner corona from $1.02 R_{\odot}$ to $2.5 R_{\odot}$ with a consistent spatial resolution of $2.5''$, a required spectral resolution of less than 40 pm, a cadence of one minute, and a polarimetric sensitivity of 10^{-3} in the polarization continuum in nominal operation. Achieving these ambitious goals is only feasible through space-based observations and the utilization of an externally occulted coronagraph. Figure 1 represents the squared field of view of CMAG superimposed on a simulated K-corona [48] brightness image derived from a magnetohydrodynamic model¹. The CMAG mission holds the potential to revolutionize our understanding of the inner corona by providing direct and precise measurements of the magnetic field and shed light on the processes underlying coronal dynamics, solar flares, and CMEs.

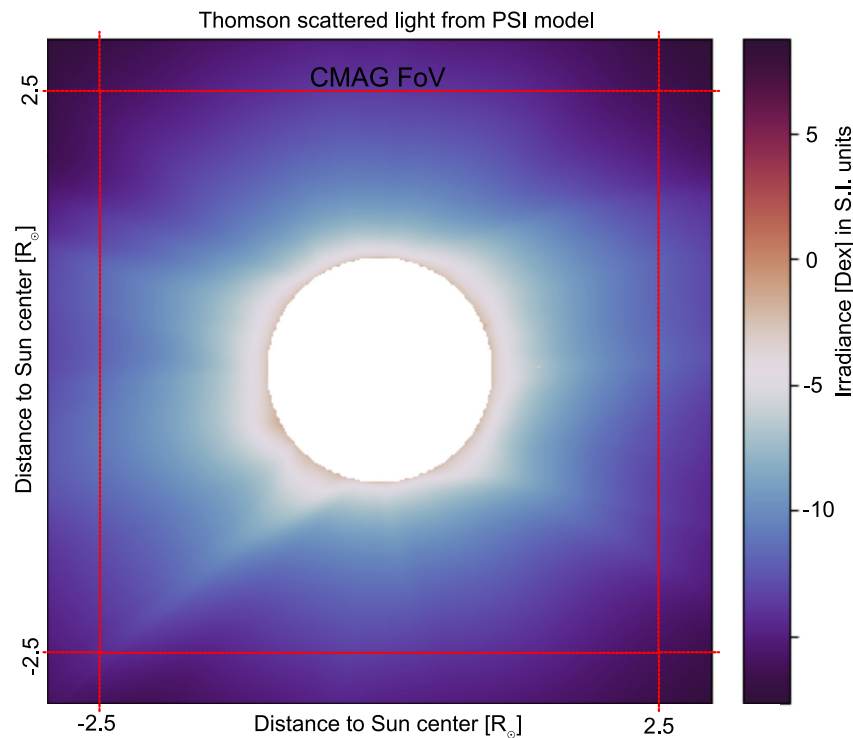


Figure 1. Simulated solar K-corona generated from a magnetohydrodynamic model. The field-of-view (red square) corresponds to $2.5 R_{\odot}$, matching that of CMAG.

1.3. Solar corona polarimetry

Nowadays, the inference of magnetic fields from spectropolarimetric measurements of the forbidden coronal lines, Fe XIV 530 nm, Fe XI 789 nm, and Fe XIII 1074 nm, has become possible with the interpretation of the Zeeman, scattering, and Hanle effects [18,38]. The Zeeman effect polarizes light from spectral lines due to the presence of magnetic fields in a moderate to strong regime. The Hanle effect, on the other hand, depolarizes light that is already polarized by scattering (or other physical mechanisms) in the presence of weak magnetic fields [24,46]. To measure polarization in coronal lines, high-precision differential photometry is mandatory, and indeed, all four Stokes parameters of solar light must be measured. Quiet coronal line intensities (Stokes I; imaging) are one order of magnitude above the K-corona intensity at $1.10 R_{\odot}$ [17]. Linear polarization signals (Stokes Q, U) are weaker, about 1 to 10% of the line core intensity, and hence subject to larger contamination by the already polarized solar corona (the so-called K-corona is linearly polarized by scattering to a large degree). Stokes V is even feebler than linear polarization (a few percent or per-mille). Linear polarization is mainly proportional to the degree of anisotropy of the incident light coming from the solar disk, which depends on the height above the Sun's visible surface at where we observe, while the Stokes V amplitude is mainly proportional to the line-of-sight component of the field.

Recent numerical models predict Stokes V amplitudes slightly above 0.1% in coronal loops for the Fe XIII @ 1074 nm line [38], in line with earlier predictions [19] that suggested amplitudes of about 0.5×10^{-3} for coronal loops and field strengths as low as 2 G. Therefore, measuring circular polarization in the corona is extremely challenging. Simple magnetographic calculations (see Figure 2) suggest signals barely above 0.1 % in the line emission of the quiet corona if the field is stronger than 10 G. Observations of magnetic fields in the inner corona are very scarce. Those we currently have, are severely limited in terms of spatial and temporal resolution. For example, Lin and collaborators [27] obtained the first observations, requiring a spatial sampling of 20 arcseconds and a temporal integration of over an hour to detect circular polarization signals in the inner corona. Recent measurements

suggest much stronger fields, in the range of 50-200 G, for cold and hot coronal loops [4,23], hence predicting larger Stokes V signals in these structures. Coronal electron densities change from 10^9 cm^{-3} at the bottom to 10^6 at $2 R_{\odot}$. Therefore, the sensitivity of measurements decreases with distance. However, in loop structures, the density reaches 10^{11} cm^{-3} , and emissivity is larger by one order of magnitude, making the signal-to-noise ratio (S/N) go up, hence increasing polarization sensitivity for equivalent exposure times. Electron density reaches 10^{12} cm^{-3} in flaring loops[34]. When more photons are available, CMAG will achieve the required polarization sensitivity in less time, with a FoV that covers from 1.02 to $2.5 R_{\odot}$, and a spatial resolution of 2.5 arcsec at 750 nm. Perhaps the most relevant aspect of the mission is that, in addition to its capabilities, it will take observations from space with unprecedented pointing stability, enabling the measurement of polarization signals in fainter solar structures. Remarkably, no existing or planned mission is able to tackle these challenging measurements, despite the efforts of the solar community over the last few decades. Solar missions with specific instrumentation for performing spectropolarimetry in the corona, such as the Solar magnetism eXplorer (SolmeX) [31] or the Magnetic Imaging of the Outer Solar Atmosphere (MImOSA) [32] missions, have been already proposed. Certainly, the CRYO-NIRSP instrument [12] will likely provide excellent data on the inner corona, although it is expected that the observations will be much more limited in terms of time and have very restricted fields of view compared to CMAG, which aims to observe the entire inner corona. Currently, there are ground-based spectropolarimetric observations of the inner corona, such as those from uCoMP, at a spatial resolution of 6 arcseconds and a field of view covering from 1.03 to 2 solar radii. Linear polarization information has already been retrieved although circular polarization still remains elusive so far.

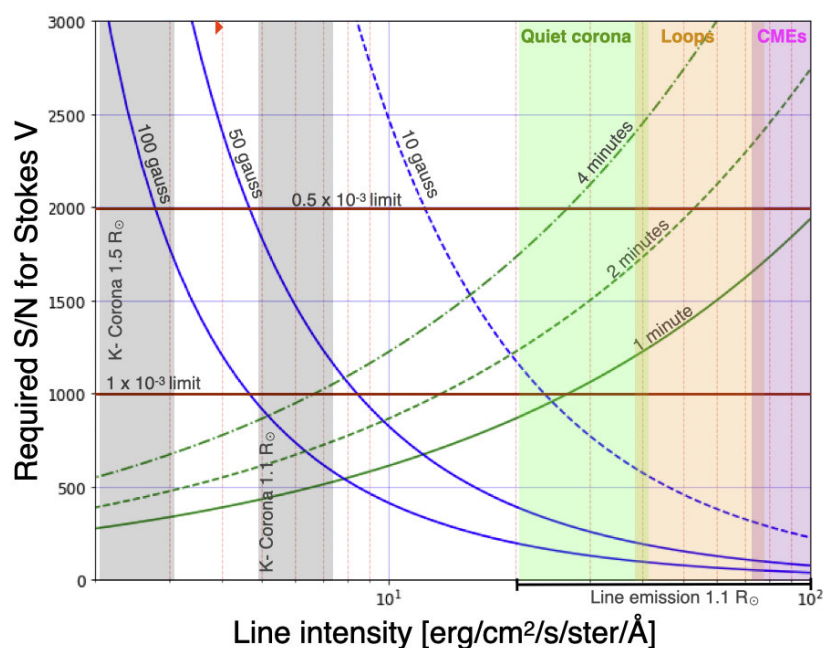


Figure 2. Detectability diagram. Calculations assume the weak field approximation on lines with a Doppler width of 20 km/s [18]. Emission intensities at different regions are represented with shaded areas. Diagram regions below blue lines indicate magnetic field strength detectability for Fe XIII @ 1074 nm and no atomic alignment. Diagram regions below green lines indicate the reached S/N in Stokes V for the given exposure times with a 10 cm aperture telescope (Table 1) at 1 au from the Sun and a total transmission of 0.4, sensor quantum efficiency of 50% and a polarimetric efficiency of 0.5.

1.4. Scientific goals of the CMAG mission

The mission aims to answer the overarching question, "How does magnetic energy transformation occur in the inner corona, driving coronal heating and all eruptive phenomena relevant to space weather effects on Earth?" This global question breaks down into specific questions described below.

1. What is the structure of the inner coronal magnetic field? Understanding the magnetic field's structuring in coronal loops and streamers and its evolution and relationship with photospheric fields is crucial. CMAG's high spatial resolution (2.5 arcsec) and cadence (≈ 1 min) will determine the strength and direction of the vector magnetic field from close to the surface to the higher layers for providing an empirical basis that help validate and refine current extrapolations and improve coronal magnetic models.
2. What is the coronal origin of the solar wind? The solar wind has distinct components: slow and fast, related to coronal streamers, coronal hole boundaries, and the solar network. CMAG will investigate the magnetic connection between coronal holes, streamers, and the solar wind, aiding to understand how the solar wind propagates through the heliosphere and its relationship with coronal waves.
3. How are flares and CMEs generated? Flares and CMEs are phenomena with different effects on the heliosphere and the Earth's environment. CMAG will reveal the inner corona's internal structure and evolution and follow the magnetic field vector during the CME onset and the generation of associated waves. At a resolution of 2.5 arcseconds, it could also provide a glimpse of the evolution of the magnetic field structure at the reconnection sites.
4. What is the origin of solar coronal heating? Measurements of magnetic field strength will provide a quantitative basis for assessing the origin of non-thermal heat observed in the Sun's inner coronal layers.
5. What is the role of the inner corona in space weather? CMAG's measurements of inner coronal magnetic fields at L5, provided in almost real-time, will greatly enhance space weather nowcasting and forecasting capabilities, crucial for predicting radiation and energetic particle impacts on Earth as a consequence of flares and CMEs.

1.5. Top science requirements

To achieve its science goals, CMAG must collect as many photons as possible to make the required measurements of all four Stokes parameters of the selected spectral line(s) for achieving the required polarimetric performance. The necessary spatial, spectral, and temporal resolutions will be possible through full vector spectropolarimetric observations using a coronal magnetograph as the sole instrument on board a spacecraft, hereafter referred to as the CMAG spacecraft. This will be combined with an external occulter installed on another spacecraft, hereafter referred to as the occulter spacecraft. These two spacecraft will maintain a formation flight distance of 430 meters for coronagraphic observations. At that distance, the radius of the occulter has to be around two meters. The observational periods will be of, at least, 2.5 hours every twelve hours¹. The main scientific and design requirements are listed in Table 1. Since polarimetry demands precise pointing stability (Performance Drift Error, PDE, must be better than 0.125" in one minute), both spacecraft will adhere to stringent requirements (see next Section).

¹ This assumes a mission to L5 and a certain solid fuel capacity that may vary.

Table 1. CMAG spacecraft main instrument baseline requirements.

Spatial resolution	2.5 arcsec at 750 nm
Aperture	10 cm
Cadence	≈ 1 min for S/N = 1000 in Stokes Q, U, and V
Field of view (FoV)	≈ 2400" (≈ 0.66° = 2.5 R _☉)
Targets spectral lines	Fe XIV 530 nm ; Fe XI 789 nm ; Fe XIII 1074 nm
Spectral resolution	20 pm ; 30 pm ; 40 pm
Maximum spectral shift over the FoV	25 pm ; 30 pm ; 50 pm
Detector dimensions	4 k × 4 k pixels
Etalon max. incidence angle ¹	1.28°
Etalon diameter	≈ 60 mm
Polarization modulator interm. image diameter	≈ 55 mm
dimensions	< 1 m ³
stray-light requirements	< 0.1 % @ 1.02 R _☉

¹ Etalons placed in collimated configuration are often slightly tilted with respect to the incident beam. The etalon tilt induce a wavelength blueshift or the etalon peak transomission across the FoV.

CMAG’s measurements complement those of METIS aboard the Solar Orbiter mission by providing access to the coronal magnetic field. While our goals are similar to those of the (on-ground) Large Coronagraph of COSMO (the COronal Solar Magnetism Observatory project [45]), we use a much smaller aperture telescope (10 cm vs. 170 cm). Nonetheless, we expect to obtain sharper coronal structure maps due to the absence of atmospheric seeing and a larger throughput, resulting in high S/N observations in less time. Moreover, externally occulted coronagraphy ensures significantly lower scattered light levels (by three orders of magnitude [37]) when the occulter is positioned at 430 m, increasing our polarimetric sensitivity and allowing us to observe much closer to the solar limb (at 1.02 R_☉) where scattered light effects are more detrimental (see Fig. 3, based on [3]).

The approved NASA’s PUNCH mission [8], expected to be launched in 2025, follows a loose formation-flying concept and aims to explore the corona and solar wind by imaging light scattered from free electrons from 6 to 180 solar radii. Missions like PUNCH will complement the science being done now with other missions such as Solar Orbiter, enabling space weather scientists to trace solar phenomena from their origin to their potential impacts on Earth. CMAG’s expected benefits will be a significant leap in this endeavor, provided that it is operational in a reasonable time to overlap with the above missions. DKIST will also benefit from pointing its extremely high spatial resolution instrumentation to targets provided by CMAG. Additionally, CMAG is expected to be a full member of the battery of instruments enabling multi-messenger solar astronomy, combining its measurements not only with remote-sensing coronagraphs but also with in-situ instruments aboard missions like Solar Orbiter and Parker Solar Probe, ushering to a new era of solar physics [28].

2. Mission concept

2.1. Mission profile

The mission consists of two spacecraft, the CMAG and the occulter spacecraft, flying in formation at the L5 Lagrangian point for a duration of 7 years. The occulter spacecraft must carry the necessary equipment for enabling formation flying, as well as the occulter disk. The CMAG spacecraft will carry the main scientific payload instrument: a coronal magnetograph. During observations, CMAG will be positioned approximately 430 meters behind the occulter, significantly reducing solar disk scattered light by at least one order of magnitude as compared to the Proba-3 mission. Figure 3 shows the relevance of a high inter-satellite distance. Unity represents the disk intensity. The regular bright profile without any instrument is plotted in green. The use of an external occulter like that in Proba-3 at about 140 m from the coronagraph reduces the levels significantly (orange). But if the occulter is at about 400 m as in the case of CMAG, the background of scattered light decreases still one more order of

magnitude, hence making it easier the observation of the solar corona in a unique way. Moreover, the diffraction effects near the limb are much better suppressed, what allows observing closer to the solar limb, much closer to the transition region of the Sun. This reduction is crucial to extract the polarimetric observations needed to measure the coronal vector magnetic field. Indeed, critical heights of CME onset and prominence instabilities take place from 1.03 to $1.1 R_{\odot}$ [16], so those heights close to the solar limb are critical to observe if one wants to follow these events at all their evolutionary stages.

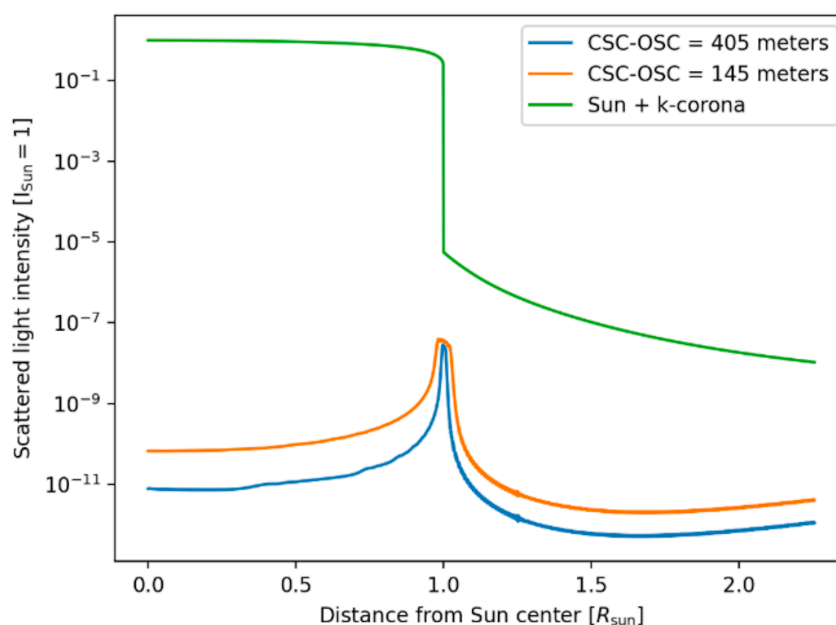


Figure 3. Solar scattered light intensity as a function of the distance to the solar disk center.

The mission's choice of the Lagrangian L5 point, which positions CMAG it at an angle of 60 degrees away from the Sun-Earth line, holds a significant advantage for solar physics and space weather research altogether. This positioning allows us to effectively identify the formation of potentially eruptive structures within the critical region of the corona, often referred to as the "danger" zone for Earth. Moreover, from this unique vantage point, we gain the capability to observe these structures during their gradual ascent in what is known as the "slow-rise phase." This level of observation and insight into solar phenomena is unattainable from the Earth-based perspective and is crucial for enhancing our understanding of solar activities that can impact our space environment. In any case, it's worth noting that the observation of magnetic fields in the inner corona from space remains a significant challenge in solar physics. Therefore, the majority of our (stand-alone) solar objectives could still be achievable from, for example, the Lagrangian L1 point.

CMAG observations can be performed simultaneously and without interference to any other instrumentation aboard the occulter spacecraft. Both spacecraft can be launched together and then transferred to the Lagrangian point. The CMAG spacecraft will travel as a small piggy-back of the main primary mission. Both will have the necessary metrology equipment to maintain the right formation flying configuration with respect to one another.

Earth-Sun system Lagrangian points, being in solar orbit, guarantee minimum propellant consumption for maintaining the formation due to their relatively small gravitational perturbations compared to any Earth-bound orbit. Preliminary analyses show that with current technology, mission performance needs can be accomplished. But in addition, several opportunities have been identified which could potentially improve this further upon design consolidation. A radio-frequency link will be implemented between both spacecrafts providing two key services: on one hand as a data link, on the other hand as a first metrology step, determining relative position thanks to

differential RF ranging technology. The main spacecraft, which also carries the occulter, will act as a communication relay to transmit the necessary CMAG data products to the Science Operation Centre. No dedicated communications transceiver between CMAG and the ground segment is necessary, although a low-bit-rate data link with the ground station is foreseen for housekeeping, telemetries, and telecommands. The primary spacecraft, which carries the two-meter radius occulter (making it the main and likely heavier of the two spacecrafts), can also accommodate remote or in-situ instrumentation. However, this does not imply that communications with the ground will be established directly from CMAG. It can be devised as a stand-alone mission, as well.

The baseline for the CMAG platform is close to a service-like module with a weight of 300 kg and a maximum power consumption of 100 W, excluding any potential structural redesign or additional propellant needs. For the Attitude and Orbit Control System (AOCS), CMAG will carry star trackers and reaction wheels for fine 3-axis-stabilized pointing mode, combined with coarse rate and Sun sensors for safe operations. A cold gas propulsion system will be used for both relative position control and reaction wheel unloading, ensuring formation flight. The CMAG spacecraft will be able to generate power when outside the occulter shadow and will have active thermal control. The battery capacity will be sized for the foreseen scientific operations, which take place within the shadow cast by the main spacecraft.

A metrology sensor suite is key for mission robustness and for achieving the required performance. Metrology must be accurate enough to meet the mission's scientific requirements and robust enough, at the same time, to guarantee recovering formation flight from a completely lost state after any potential system failure and a smooth handover between the two spacecraft. Four key elements make these operations seamless: the Formation Flying Radio Frequency (FFRF) metrology, based on differential RF ranging from a reduced set of antennas, provides almost omnidirectional coverage with comparatively low accuracy; the Visual Based System (VBS), placed on the occulter spacecraft and always pointing away from the Sun direction, can detect a light pattern on CMAG and is capable of robustly providing lateral relative position estimation with relatively high accuracy, as well as coarse longitudinal estimation while maintaining a wide enough field of view to allow for both the Science and the Stand-By modes (see below); the Fine Longitudinal System (FLS) laser-based metrology that reflects on a corner-cube retro-reflector on the occulter spacecraft and provides high-accuracy longitudinal estimation; and the Shadow Position Sensor (SPS), a limb detector that corrects the lateral positioning of the CMAG spacecraft with respect to the occulter shadow. The last two systems guarantee a spacecraft positioning within a 1 mm error margin in the perpendicular plane (lateral) to the line-of-sight and along it (longitudinal). Relative positioning stability (lateral) will be 0.3 mm while the absolute pointing error and stability are 2.5 arcseconds and 1 arcsecond in 1 minute, respectively.

2.2. Mission operations baseline and spacecraft concept

CMAG would be launched in a stacked configuration, piggy-backing on the occulter spacecraft. It will be commissioned during the initial stages of the transfer to the Lagrangian point. After arrival, formation flying commissioning and calibration will take place. The CMAG operational phase will comprise three stages (see Figure 4): Science Mode (SM), Stand-By Mode (SBM), and Parking Mode (PM). During SM, CMAG will position the instrument aperture at the necessary location within the occulter shadow and perform station-keeping with high accuracy, using the highest precision elements in the AOCS and metrology chain, and a propulsion system. As the occulter limits the solar panel's power, the shadow time will be limited to the energy storage capacity. Preliminary estimates suggest a duration of approximately 2.5 hours until battery depletion.

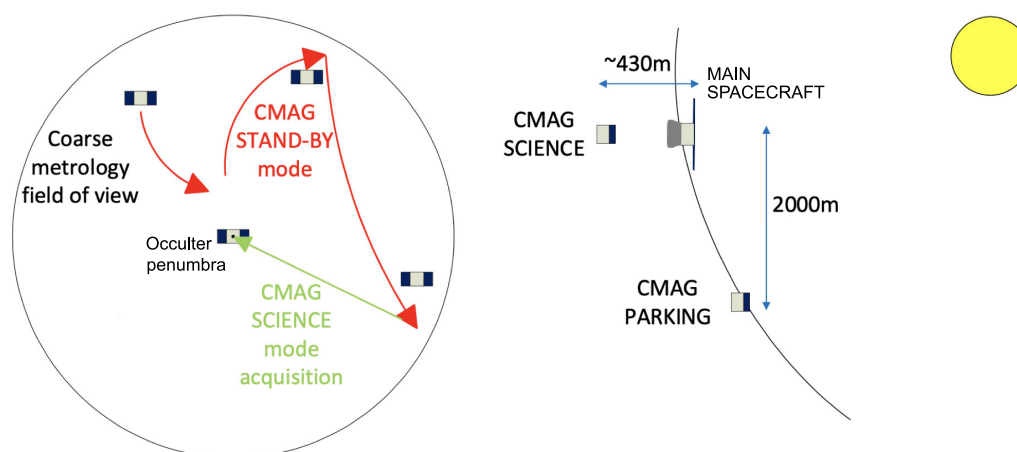


Figure 4. CMAG concept of operations. Autonomous operations (left) and non-operational orbit (right).

SBM is needed to optimize mission resources when not performing fine position control. The spacecraft will exit the shadow region to charge the battery while remaining within the coarse metrology's operational range to ensure a swift transition back to fine positioning when needed. This mode also allows for propellant saving, since the positioning requirements are much less stringent. The current re-charging time estimation is seven hours. A 9.5-hour SBM period will then allow for a 12-hour observation cycle, making it easier to synchronize CMAG's observations with the ground segment. PM ensures safety against collision for extended periods, although the Lagrangian points already ensure safe and simple operations without collision risk. PM allows CMAG a long-term, passive relative orbit for commissioning, fault recovery, or maintenance. PM can be entered when commanded from the ground. SM and SBM will be fixed and defined by design, autonomously managed by the CMAG spacecraft without operator intervention. The proposed design baselines two observational cycles per day, representing the worst-case scenario, with each cycle providing 2.5 hours of scientific operations.

2.3. Payload concept design

The proposed CMAG instrument is an imaging spectropolarimeter that measures all four Stokes parameters at given wavelength samples of selected emission spectral lines from the corona: Fe XIV 530 nm, Fe XI 789 nm, and Fe XIII 1074 nm. These spectral lines are among the ones showing the largest intensity above the K-corona. No other mission aims at carrying out vector magnetography and map the LOS and plane-of-the-sky velocities of the highly dynamic inner corona. The baseline design (see Figure 5), with an entrance pupil diameter of 10 cm, combines the first stage of the full disk telescope from the Polarimetric and Helioseismic Imager (PHI)[40] instrument aboard Solar Orbiter with the conceptual design of the TuMag magnetograph [9] for the SUNRISE III mission [39]. Two athermalized doublets focus the Sun on an intermediate focal plane. A field lens placed before that focal plane re-images the entrance pupil to infinity to make the image telecentric. The doublets are optimized to produce the best image of the external occulter where an internal occulter is placed. A polarization modulation package (PMP) based on Liquid Crystal Variable Retarders (LCVRs) carries out the polarization modulation right after a filter wheel containing three pre-filters corresponding to the three target spectral lines. A collimator, consisting of a telephoto system to reduce the total track of the instrument, re-images the Sun onto infinity and focuses the pupil on its image focal plane, where the etalon and the Lyot stop are placed. Finally, a camera telephoto system refocuses the image onto the detector with a fixed spatial sampling of 1.25'' (2.5'' resolution). If the size limitations of the instrument allow it, the camera system shall provide a telecentric image.

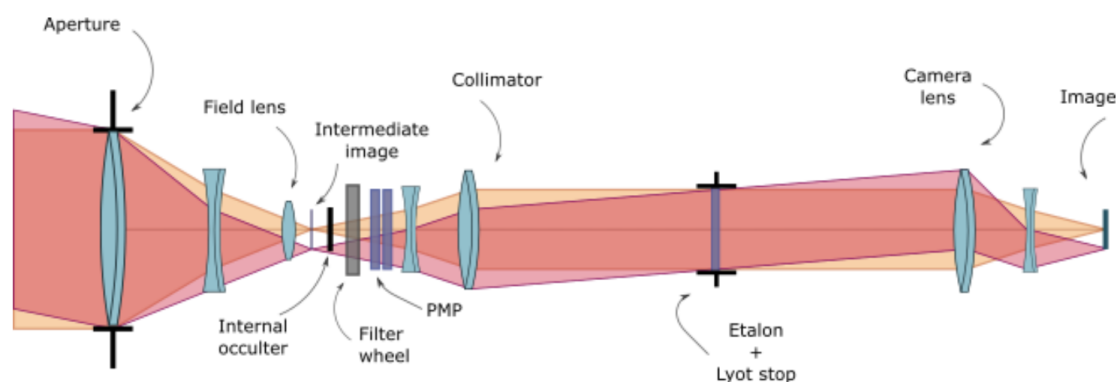


Figure 5. CMAG coronagraph instrument concept.

The instrument electronics include: a Data Processing Unit (DPU) for the overall control of the instrument and data processing, communications with the S/C, carrying out the main processing functionalities, and sufficient storage to keep 2.5 hours worth of scientific data; an Analog, Mechanism and Heater Drivers board (AMHD); a High Voltage Power Supply (HVPS) for tuning the etalon; a Power Converter Module (PCM); and an Electrical Distribution System (EDS). The DPU is the core of the instrument electronics and has to be tailored to perform data acquisition and accumulation, demodulation, retrieval of the different sub-products (see Sect. 3.5), and compression. The AMHD will be in charge of synchronizing the PMPs and the etalon, taking care of the thermal stabilization of the more critical elements, and managing housekeeping data for the overall control of the instrument, among other analog tasks. The PCM is the direct interface to the platform and should hence fulfill the necessary requirements and redundancy. The spacecraft will have image stabilization capabilities to guarantee the required $0.125''$ PDE stability in one minute. The E-unit will be equipped with the necessary firmware (heritage of the Solar Orbiter PHI instrument complex on-board data processing) to provide the required data products. On-board pre-processing of payload data will be key for the reduction of the downlink telemetry.

2.4. CMAG data products

The instrument will observe the full Stokes vector in several wavelength samples across the aforementioned coronal lines. For transforming the observations into scientific data products, most of them will be processed in the DPU, including dark and flat-fielding corrections, demodulation, normalization, and subsequent transformation to scientific products, minimizing telemetry usage. The expected data products are maps of polarization brightness (K-corona), line-of-sight plasma velocity component, line Doppler widths, the total line polarization, the (non-disambiguated) orientation of the magnetic field vector, and the amplitude and sign of Stokes V. The latter two products can readily be calculated from the linear polarization signals and from the circular polarization (using the weak field approximation) since the lines lie in the strong limit of the Hanle effect [6,24] in optically thin coronal plasma at locations where circular polarization is above the noise level of 10^{-3} . To increase the polarimetric sensitivity, longer integration times (by adding datasets, reducing spatial resolution, or increasing exposure time) are foreseen in well-defined cases. Inferring the full magnetic field vector requires downloading raw or pre-processed data since, for fully interpreting optically thin forbidden coronal lines, collisional excitation and resonance scattering. Other products will be determined on the ground, e.g., coronal density maps can be inferred from the polarization brightness. Intermediate products are also foreseen. For instance, brightness temperatures can also be inferred provided the spectral line profile is available. CMAG will also provide forward modeling tools for the interpretation of the products on the ground and for aiding field extrapolations and modeling of the solar corona.

3. A mission opportunity

CMAG mission was proposed to ESA in February 2022 in response to the ESA’s call for “Fast” mission opportunity. In that proposal, the main platform was assumed to be the current ESA’s Space Safety Vigil mission, which, with a few configuration modifications and additional equipment, can act as an external occulter and enable formation flying. The combination with the Vigil mission at the L5 Lagrangian vantage point ensures a unique, low-risk, cost-effective and interdisciplinary scientific return considerably improving current coronal models and space weather predictions in a clear benefit for both the Science and the Space Safety programs of ESA.

The use of Vigil as an external occulter presented an exceptional opportunity for the solar physics and space weather communities, as it allows establishing a connection between photospheric magnetic activity (observed with the Photospheric Magnetic Field Imager instrument, PMI, aboard Vigil; [41]) and the corona through CMAG’s continuous monitoring of the magnetic field and plasma velocities in the inner corona. Combining CMAG with Vigil’s solar instrumentation ensures optimal scientific return and increased space weather forecasting capabilities, which are not expected from any other space agency in the near future, resulting in a significant qualitative leap.

However, CMAG can be adapted to any other space mission, provided it fulfills the science requirements. Modifications to the main mission will be necessary. The main spacecraft needs to carry an occulter disk, which can come from redesigned solar panels or a retractable structure, ensuring the mission’s remote sensing payload remains unperturbed. The inter-satellite distance, estimated to be 430 m, requires a 2 m disk radius. The metrology suite of instruments for formation flight does not necessarily interfere with the main AOCS system design, resulting in an estimated total mass increment of 24 kg, including the occulter disk. CMAG can be used as a science data relay, transmitting data through an inter-satellite link to the main mission, which downloads them to the Ground Station. Operationally, CMAG observations will be performed autonomously, providing the necessary data products. It can also be used on demand if the scientific team needs particular observations.

Funding: This work has been funded by AEI/MCIN/10.13039/ 501100011033/ (RTI2018-096886-C5, PID2021-125325OB-C5, PCI2022-135009-2) and ERDF “A way of making Europe”; “Center of Excellence Severo Ochoa” awards to IAA-CSIC (SEV-2017-0709, CEX2021-001131-S); Plan Andaluz de Investigación, Desarrollo e Innovación (PAIDI 2020) P20_01307; and a Ramón y Cajal fellowship awarded to DOS. DML is grateful to the Science Technology and Facilities Council for the award of an Ernest Rutherford Fellowship (ST/R003246/1).

Acknowledgments: Not for the moment

Conflicts of Interest: The authors declare no conflict of interest. The funders had no role in the design of the study; in the collection, analyses, or interpretation of data; in the writing of the manuscript; or in the decision to publish the results.

Abbreviations

Abbreviations

The following abbreviations are used in this manuscript:

CMAG	Coronal Magnetograph
ESA	European Space Agency
CME	Coronal Mass Ejection
MHD	Magnetohydrodynamic
LASCO	Large Angle and Spectrometric Coronagraph
UVCS	Ultraviolet Coronagraph Spectrometer
SOHO	Solar and Heliospheric Observatory
STEREO	Solar TERrestrial RELations Observatory
SECCHI	Sun-Earth Connection Coronal and Heliospheric Investigation
METIS	the multi-wavelength coronagraph for the Solar Orbiter mission
SoloHI	Solar Orbiter Heliospheric Imager
ASPIICS	Association of Spacecraft for Polarimetric and Imaging Investigation of the Corona of the Sun
CRYO-NIRSP	Cryogenic Near-IR Spectro-Polarimeter

DKIST	Daniel K. Inouye Solar Telescope
SPARK	Solar Particle Acceleration Radiation and Kinetics
PDE	Performance Drift Error
COSMO	COronal Solar Magnetism Observatory
NASA	National Aeronautics and Space Administration
PUNCH	Polarimeter to Unify the Corona and Heliosphere
AOCS	Attitude and Orbit Control Subsystem
PHI	Polarimetric and Helioseismic Imager
TuMAG	Tunable Magnetograph

Notes

¹ Predictive Science Inc. <https://www.predsai.com/portal/home.php>

References

1. Antonucci, E., Romoli, M., Andretta, V., et al. 2020, 642, A10. doi:10.1051/0004-6361/201935338

2. Aschwanden, M. J. 2005, Physics of the Solar Corona. An Introduction with Problems and Solutions (2nd edition), by M.J. Aschwanden. 892 pages. ISBN 3-540-30765-6, Library of Congress Control Number: 2005937065. Praxis Publishing Ltd., Chichester, UK; Springer, New York, Berlin, 2005.

3. Bout, M., Lamy, P., Maucherat, A., et al. 2000, 39, 3955. doi:10.1364/AO.39.003955

4. Brooks, D. H., Warren, H. P., & Landi, E. 2021, 915, L24. doi:10.3847/2041-8213/ac0c84

5. Brueckner, G. E., Howard, R. A., Koomen, M. J., et al. 1995, 162, 357. doi:10.1007/BF00733434

6. Casini, R., White, S. M., & Judge, P. G. 2017, 210, 145. doi:10.1007/s11214-017-0400-6

7. Culhane, J. L., Harra, L. K., James, A. M., et al. 2007, 243, 19. doi:10.1007/s01007-007-0293-1

8. Deforest, C., Killough, R., Gibson, S., et al. 2022, 2022 IEEE Aerospace Conference, 11. doi:10.1109/AERO53065.2022.9843340

9. Del Toro Iniesta, J. C., Orozco Suárez, D., Álvarez-Herrero, A. et al. 2024, in preparation.

10. Domingo, V., Fleck, B., & Poland, A. I. 1994, 70, 7. doi:10.1007/BF00777835

11. Erdélyi, R. & Fedun, V. 2007, Science, 318, 1572. doi:10.1126/science.1153006

12. Fehlmann, A., Kuhn, J. R., Schad, T. A., et al. 2023, 298, 5. doi:10.1007/s11207-022-02098-y

13. Galano, D., Bemporad, A., Buckley, S., et al. 2018, 10698, 106982Y. doi:10.1117/12.2312493

14. Howard, R. A., Moses, J. D., Vourlidas, A., et al. 2008, 136, 67. doi:10.1007/s11214-008-9341-4

15. Howard, R. A., Vourlidas, A., Colaninno, R. C., et al. 2020, 642, A13. doi:10.1051/0004-6361/201935202

16. James, A. W., Williams, D. R., & O’Kane, J. 2022, 665, A37. doi:10.1051/0004-6361/202142910

17. Judge, P. G. 1998, 500, 1009. doi:10.1086/305775

18. Judge, P. G., Casini, R., Tomczyk, S., et al. 2001, Technical Report, PB2002-102493; NCAR/TN-466-STR, 02

19. Judge, P. G. & Casini, R. 2001, Advanced Solar Polarimetry – Theory, Observation, and Instrumentation, 236, 503

20. Judge, P. G., Hutton, R., Li, W., et al. 2016, 833, 185. doi:10.3847/1538-4357/833/2/185

21. Kohl, J. L., Esser, R., Gardner, L. D., et al. 1995, 162, 313. doi:10.1007/BF00733433

22. Kosugi, T., Matsuzaki, K., Sakao, T., et al. 2007, 243, 3. doi:10.1007/s11207-007-9014-6

23. Kuridze, D., Mathioudakis, M., Morgan, H., et al. 2019, 874, 126. doi:10.3847/1538-4357/ab08e9

24. Landi Degl’Innocenti, E. & Landolfi, M. 2004, Polarization in Spectral Lines. By Egidio Landi Degl’Innocenti and Marco Landolfi, University of Fierenze, Firenze, Italy; Arcetri Observatory, Firenze, Italy. ASTROPHYSICS AND SPACE LIBRARY Volume 307 Kluwer Academic Publishers, Dordrecht. doi:10.1007/978-1-4020-2415-3

25. Li, W., Grumer, J., Yang, Y., et al. 2015, 807, 69. doi:10.1088/0004-637X/807/1/69

26. Li, W., Yang, Y., Tu, B., et al. 2016, 826, 219. doi:10.3847/0004-637X/826/2/219

27. Lin, H., Kuhn, J. R., & Coulter, R. 2004, 613, L177. doi:10.1086/425217

28. Martinez Pillet, V., Tritschler, A., Harra, L., et al. 2020, arXiv:2004.08632. doi:10.48550/arXiv.2004.08632

29. Mathioudakis, M., Jess, D. B., & Erdélyi, R. 2013, 175, 1. doi:10.1007/s11214-012-9944-7

30. Müller, D., St. Cyr, O. C., Zouganelis, I., et al. 2020, 642, A1. doi:10.1051/0004-6361/202038467

31. Peter, H., Abbo, L., Andretta, V., et al. 2012, Experimental Astronomy, 33, 271. doi:10.1007/s10686-011-9271-0

32. Peter, H., Ballester, E. A., Andretta, V., et al. 2022, *Experimental Astronomy*, 54, 185. doi:10.1007/s10686-021-09774-0
33. Raouafi, N. E., Matteini, L., Squire, J., et al. 2023, 219, 8. doi:10.1007/s11214-023-00952-4
34. Reale, F. 2014, *Living Reviews in Solar Physics*, 11, 4. doi:10.12942/lrsp-2014-4
35. Hamish A. S. Reid, et al. 2024, *The Solar Particle Acceleration Radiation and Kinetics (SPARK) mission concept*, MDPI, same edition
36. Rimmele, T. R., Warner, M., Keil, S. L., et al. 2020, 295, 172. doi:10.1007/s11207-020-01736-7
37. Rougeot, R., Flamary, R., Galano, D., et al. 2017, 599, A2. doi:10.1051/0004-6361/201629259
38. Schad, T. & Dima, G. 2020, 295, 98. doi:10.1007/s11207-020-01669-1
39. Solanki, S. K. et al. 2024, in preparation.
40. Solanki, S. K., del Toro Iniesta, J. C., Woch, J., et al. 2020, 642, A11. doi:10.1051/0004-6361/201935325
41. Staub, J., Fernandez-Rico, G., Gandorfer, A., et al. 2020, *Journal of Space Weather and Space Climate*, 10, 54. doi:10.1051/swsc/2020059
42. Temmer, M. 2021, *Living Reviews in Solar Physics*, 18, 4. doi:10.1007/s41116-021-00030-3
43. Tomczyk, S., Card, G. L., Darnell, T., et al. 2008, 247, 411. doi:10.1007/s11207-007-9103-6
44. Tomczyk, S. & Landi, E. 2019, *Solar Heliospheric and INterplanetary Environment (SHINE 2019)*
45. Tomczyk, S., Burkepile, J., Casini, R., et al. 2023, doi:10.3847/25c2cfef.de9518e7
46. Trujillo Bueno, J. 2001, *Advanced Solar Polarimetry – Theory, Observation, and Instrumentation*, 236, 161. doi:10.48550/arXiv.astro-ph/0202328
47. Trujillo Bueno, J. & del Pino Alemán, T. 2022, 60, 415. doi:10.1146/annurev-astro-041122-031043
48. Computation of the Thomson scattering of the K-Corona. Available online: <https://github.com/aliciavr/thomsonpy>.
49. Vourlidas, A., Howard, R. A., Plunkett, S. P., et al. 2016, 204, 83. doi:10.1007/s11214-014-0114-y
50. Yang, Z., Bethge, C., Tian, H., et al. 2020, *Science*, 369, 694. doi:10.1126/science.abb4462

Disclaimer/Publisher's Note: The statements, opinions and data contained in all publications are solely those of the individual author(s) and contributor(s) and not of MDPI and/or the editor(s). MDPI and/or the editor(s) disclaim responsibility for any injury to people or property resulting from any ideas, methods, instructions or products referred to in the content.